Award Number: W81XWH-14-1-0317

TITLE: Genetic and Diagnostic Biomarker Development in ASD Toddlers Using Resting State Functional MRI

PRINCIPAL INVESTIGATOR: Dr. Eric Courchesne

CONTRACTING ORGANIZATION: University of California San Diego
La Jolla CA, 92093

REPORT DATE: November 2017

TYPE OF REPORT: Final

PREPARED FOR: U.S. Army Medical Research and Materiel Command
Fort Detrick, Maryland 21702-5012

REPORT DOCUMENTATION PAGE

Form Approved
OMB No. 0704-0188

1. REPORT DATE	2. REPORT TYPE	3. DATES COVERED
November 2017	Final	1 September 2014 - 31 August 2017

4. TITLE AND SUBTITLE

Genetic and Diagnostic Biomarker Development in ASD Toddlers Using Resting State Functional MRI

5a. CONTRACT NUMBER

5b. GRANT NUMBER
W81XWH-14-1-0317

5c. PROGRAM ELEMENT NUMBER

6. AUTHOR(S)

Dr. Eric Courchesne

Email: ecourchesne@ucsd.edu

5d. PROJECT NUMBER

5e. TASK NUMBER

5f. WORK UNIT NUMBER

7. PERFORMING ORGANIZATION NAME(S) AND ADDRESS(ES)

Univ. of California San Diego
9500 Gilman Dr
La Jolla CA, 92093

8. PERFORMING ORGANIZATION REPORT NUMBER

9. SPONSORING / MONITORING AGENCY NAME(S) AND ADDRESS(ES)

U.S. Army Medical Research and Materiel Command
Fort Detrick, Maryland 21702-5012

10. SPONSOR/MONITOR'S ACRONYM(S)

11. SPONSOR/MONITOR'S REPORT NUMBER(S)

12. DISTRIBUTION / AVAILABILITY STATEMENT

Approved for Public Release; Distribution Unlimited

13. SUPPLEMENTARY NOTES

14. ABSTRACT

Resting state fMRI and analyses of intrinsic functional networks are powerful tools for characterizing functional networks in pediatric and clinical populations. In control infants and toddlers who are scanned during natural sleep, fMRI has been used to characterize the typical development of intrinsic functional networks during resting states. Autism spectrum disorder (ASD) begins prenatal, and early maldevelopment is present in many sites and systems that mediate intrinsic network function. These networks have been little studied in ASD infants and toddlers. Our project appears to be among the first to do so. In this project N=96 ASD and typical infants and toddlers were studied; analyses of intrinsic networks provided evidence of significant and widespread disruptions in functional networks in ASD that are crucial for social, communication, cognitive, attention and salience functions. These are among the first-ever studies of the intrinsic connectivity patterns in infants and toddlers with ASD at the age of first clinical identification. The knowledge provided by our studies in combination with those of Co-PIs Dr. Fox and Dr. Glahn could open new avenues of basic genomic and animal model research that elucidate the biological bases of aberrant intrinsic network development in ASD and may identify early diagnostic, prognostic and treatment-responsiveness biomarkers of ASD.

15. SUBJECT TERMS

Nothing listed

16. SECURITY CLASSIFICATION OF:			17. LIMITATION OF ABSTRACT	18. NUMBER OF PAGES	19a. NAME OF RESPONSIBLE PERSON
a. REPORT	b. ABSTRACT	c. THIS PAGE			USAMRMC
Unclassified	Unclassified	Unclassified	Unclassified	24	19b. TELEPHONE NUMBER *(include area code)*

```

## Table of Contents

**Page**



**Appendices A, B, C attached as separate pdf files**
```

1. INTRODUCTION

Resting state functional magnetic resonance imaging (rsFMRI) and the analysis of intrinsic functional connectivity are powerful tools for characterizing functional networks in pediatric and clinical populations. In infants and toddlers who are scanned during natural sleep, rsFMRI has been used to characterize the development of intrinsic functional networks during resting states [1-6]. Not only has this body of work revealed that disruptions in early development, such as pre-term birth, can result in measurable changes in these intrinsic networks [1,4], but it has also shown, perhaps surprisingly, that the majority of them are fully or mostly formed by age 2 [6-9]. Furthermore, intrinsic *sensory* networks seem to emerge earliest and present adult-like topology by birth, while intrinsic networks involved in higher order functions merge later. Specifically, the *default mode network* (DMN) and the *dorsal attention network* (DAN) emerge by age 1 and the *salience and fronto-parietal control networks* emerge by ages 1-2 [8,9]. Moreover, by age 1 year, the DMN and DAN (also known as the task-negative and task-positive networks due to their relative deactivation and activation while performing a cognitive task) demonstrate their characteristic anticorrelated relationship and these anticorrelations increase in the second year of life [8,9]. After infancy and toddlerhood, these various networks become further refined and the relationships between them change.

As we show in our DoD-supported review (Courchesne et al, submitted; see Appendix C, new cellular, molecular and genomic evidence indicates autism spectrum disorder (ASD) begins prenatally, most likely by or before the late second trimester [10-15] as do ASD animal model studies [16-18]. Prenatal maldevelopment in ASD involves dorsolateral and mesial prefrontal, temporal, parietal and occipital cortex and amygdala and cerebellum [19] (Courchesne et al, submitted; see Appendix C). These are among the key structures that mediate the normal development and function of the higher-order intrinsic networks described above, such as DMN and DAN, as well as development of visual and auditory sensory systems that are supposed to be regulated by DMN and DAN. New diffusion tensor imaging (DTI) and activation-based fMRI from the Courchesne lab report the presence of structural and functional abnormality in these structures by ages 1 to 2 years in ASD [20-25]. Therefore, we hypothesize that the early neural maldevelopment of these key structures disrupts the normal formation and function of these important higher-order intrinsic networks, which underlie social, communication, cognitive and attention functions. Remarkably, these networks have not been well studied in ASD at the earliest ages. This is a major gap in basic and clinical knowledge. Such knowledge could open new avenues of basic genomic and animal model research that can elucidate the developmental neural biological bases of ASD and early clinical diagnostic and prognostic biomarker research.

The Courchesne lab has gathered the largest existent sample of resting state fMRI data from ASD infants and toddlers. In addition, we have gathered complementary and independent neurobehavioral evidence from our GeoPref Test of ASD about social interest and attention deficits; this has enabled us to more directly identify which resting state fMRI networks are most related to the social deficits of ASD in at young ages. With this invaluable resource, we will identify early developmental patterns of intrinsic functional network abnormalities in ASD infants and toddlers as compared with typically developing (TD) controls. Because the Courchesne lab routinely also collects longitudinal clinical data from all infants and toddlers, analyses also investigate whether there may be subtypes of abnormal intrinsic connectivity patterns based on early clinical presentation and/or on later clinical outcome, such as social outcome by ages 3 to 4 years.

2. KEYWORDS

Autism spectrum disorder, ASD, early brain development, intrinsic functional brain networks, fMRI, infants, toddlers, clinical presentation, clinical outcome, default mode network, biomarker

3. ACCOMPLISHMENTS

What were the major goals at the UC San Diego Site during this FINAL year?

a) <u>Completing and Submitting Two Major Resting State fMRI Manuscripts on ASD Toddlers</u>

We completed and submitted two excellent manuscripts on resting state fMRI abnormalities in ASD toddlers. One was in progress the previous year and is now complete and attached (Datko et al submitted, see Appendix A) and the second we completed this past year and it too is submitted for publication and is attached (Lombardo et al. submitted; see Appendix B). In addition, this DoD grant also supported our writing of a major review article on the neural and genomic bases of ASD, which is also submitted and attached (Courchesne et al., submitted; see Appendix C).

b) Specific Aim 2 (UC San Diego Site):

i. <u>Major Task 1: ASD MRI Data Pre-Processing (Subtasks 1 and 2)</u>. Subtask 1 was to preprocess all MRI structural data. Previously, this had been done for some subjects using FreeSurfer version 5.1, and we have reprocessed the original data plus newer data, amounting to a total of 612 MRI scans. Subtask 2 was to preprocess all resting state fMRI data and has been completed for N=331 total subject scans. Many scans from that dataset are from subjects who

were not clearly ASD or TD, but had other diagnoses such as developmental delay, typical sibling of another ASD individual, or language delay. For the fMRI connectivity analyses in Datko et al (submitted; see Appendix A) reported below, 9 subjects whose data is in our first set of intrinsic connectivity analyses (see below). Milestone #1 under this Task 1 (data pre-processing of this n=98 subject fMRI and MRI dataset) was accomplished by March 2016. (see section **5. Changes**). For the fMRI connectivity analyses in Lombardo et al (submitted; see Appendix B), we studies n=195 infants and toddlers.

ii. <u>Major Task 2: Intrinsic Connectivity Analyses in ASD and TD Subjects</u>. This Milestone #2 has been completed. This past year we finalized and wrote up results from connectivity analyses in ASD and TD subjects in two manuscripts as described **next in subsection b**., below. All analyses are complete and reported in these two manuscripts.

c). What was accomplished under these goals at the UC San Diego Site?

In Datko et al. (submitted; see Appendix A), for our initial resting state fMRI analyses of intrinsic networks, we used data from 49 ASD and 49 TD infants and toddlers.

In Lombardo et al. (submitted; see Appendix B), we used fMRI date and behavioral data from n=195 ASD and control infants and toddlers.

The following sections describe design and results of these two studies aiming to identify aberrant intrinsic connectivity patterns in ASD at the age of first clinical detection and their relationships to ASD behavioral developmental abnormalities:

DATKO ET AL STUDY
(submitted, see manuscript in Appendix A; references in this section in Appendix A)

Manuscript Abstract

Atypical neural network connectivity patterns observed in adults with autism spectrum disorder (ASD) may begin much earlier in development, as suggested by a few functional MRI (fMRI) studies of ASD in late childhood. It is unknown, however, how complex network connectivity dynamics in ASD at the early age of initial clinical onset may differ from typically developing (TD) toddlers. Using resting state fMRI, we compared early-age brain network connectivity between 49 ASD and 49 matched TD toddlers (mean, 26.5 months). We used a novel method for measuring abnormal connectivity bias within and between nine large-scale networks, including social, attention and sensory. Within-network connectivity and between-network connectivity were calculated for each network and within-network bias was calculated as the percentage of the total strength of all of its connections (within-network plus between-network) attributable to its within-network connections. We tested for interactions between within-network bias, age, and group (ASD vs TD) across the nine networks. Seed-based graph components that differentiated the groups were also explored. ASD showed significantly higher within-network bias across all networks combined compared to TD. The groups showed divergent age-related trajectories such that ASD showed abnormally higher within-network bias with increasing age suggesting more isolated within-network activity and reduced between-network interaction, whereas TD trended lower with age indicating maturing between-network communication. We additionally found a graph component consisting of 22 node-to-node connections between 20 seed regions, primarily from default mode social networks and visual networks, in which ASD showed significantly lower connectivity compared to TD. This second, independent approach also revealed evidence for hypoconnectivity between default mode social and visual networks, and a global bias towards within-network connectivity in ASD toddlers. Here, using novel as well as standard methods for measuring neural connectivity, we discovered that at the age of initial clinical detection, ASD toddlers have a more immature bias towards within-network connectivity that worsens from ages 1 to 4 years in sensory, motor, attention, language, social cognition and self/other neural networks. This bias towards more isolated network activity bias may be detrimental to early-age social and communicative development as well as to top-down control of sensory perception, attention and behavioral selection that necessarily depend on large scale network interaction.

Subjects

Subjects were 49 ASD and 49 TD one-to-one gender- and age- matched infants and toddlers. Each group contained 17/49 (35%) females. The ages ranged from 13.2 to 44.5 months with a mean of 26.5 months (SD=8.9 months) in All subjects received a battery of psychological tests and final diagnoses were confirmed by licensed clinical psychologists at the Courchesne lab.

MRI Structural Imaging

To obtain multiple neuroanatomical surface and volumetric measures, all subjects received a T1-weighted anatomical scan with 1x1x1mm isotropic voxels. Our processing pipeline produces multiple detailed anatomic measures (e.g., regional cortical gradients of gray matter (GM), surface area (SA), gyrification index (GI), thickness and volumes of white matter (WM), volumes of cerebellar GM and WM, GM volumes of amygdala and striatum). It uses a combination of FSL, BrainVisa and FreeSurfer for accurate measurement of brains as young as 12 months and allows for easy identification of errors due to automated large batch processing. We used FSL's FLIRT to register the brains to a custom template consisting of an infant brain that has been registered into MNI space. GM, WM and CSF were segmented with FSL's FAST algorithm. We modified the algorithm to use partial volumes of voxels rather than neighboring voxels in order to accurately segment the small white matter tracts in temporal lobe and partial volumes of sulcal CSF at this early stage in brain development when white matter tracts are not yet robust enough to be picked up by traditional segmentation algorithms. A Matlab algorithm, adaptive disconnection, then parcellated the brain into cerebral hemispheres, cerebellar hemispheres, and brainstem. Cerebral and cerebellar hemispheres and subcortical structures entered separate processing streams. Subcortical structures were automatically identified and quantified in FreeSurfer. Cerebral hemispheres and sulci were reconstructed in BrainVisa and recombined with the original FSL segmentation to reconstruct the original surface morphology of each child's cortex. Each subject's individual anatomy was used to identify cortical subregions for measurement, allowing for measurement of unusual folding and hypergyrification. The method was optimized for measurement of surface area within the tight sulci of the infant brain and can be applied to unusually large as well as unusually small cortex.

Resting State Imaging

Our highly successful natural sleep neuroimaging procedure was used to acquire fMRI and MRI data at UC San Diego RIL Center. Key features of the procedure include mild sleep deprivation on the preceding night, vigorous physical activity on scan day, and scans that commence one hour past normal bedtime. Once asleep in the scan room weighted blankets and gradual habituation to scanner noises were used to promote continued sleep. Scanning began about 10 minutes after sleep onset and lasted approximately 30 minutes. In the first published sleep MRI-EEG study of toddlers and young children, Drs. Fox, Courchesne and Manning demonstrated that children go into Stage 3 slow wave sleep within the first 5-10 minutes after nighttime sleep onset, and stay in that stage for about 45 min, thus allowing ample time for data collection while within a single sleep stage. Resting state fMRI was conducted with a 1.5T GE scanner using a T2*-weighted EPI sequence with the following parameters: TR = 2.5 s, TE = 30 msec, voxel size of 4 x 4 x 4 mm. The scan lasted for 6 minutes and 25 seconds in the absence of any stimulation, and 154 volumes were acquired.

Data Analysis

Preprocessing of the resting state data was split into two components; core preprocessing and denoising. Core preprocessing is implemented with AFNI (http://afni.nimh.nih.gov/) using the tool speedypp.py (http://bit.ly/23u2vZp) written by Prantik Kundu (Kundu et al., 2012, Neuroimage). This core preprocessing pipeline included the following steps: (i) slice acquisition correction using heptic (7th order) Lagrange polynomial interpolation; (ii) rigid-body head movement correction to the first frame of data, using quintic (5th order) polynomial interpolation to estimate the realignment parameters (3 displacements and 3 rotations); (iii) obliquity transform to the structural image; (iv) affine co-registration to the skull-stripped structural image using a gray matter mask; (v) nonlinear warping to MNI space (MNI152 template) with AFNI 3dQwarp; (v) spatial smoothing (6 mm FWHM); and (vi) a within-run intensity normalization to a whole-brain median of 1000. Core preprocessing was followed by denoising steps to further remove motion-related and other artifacts. Denoising steps included: (vii) wavelet time series despiking ('wavelet denoising'); (viii) confound signal regression including the 6 motion parameters estimated in (ii), their first order temporal derivatives, and ventricular cerebrospinal fluid (CSF) signal (referred to as 13-parameter regression). The wavelet denoising method has been shown to mitigate substantial spatial and temporal heterogeneity in motion-related artifact that manifests linearly or non-linearly and can do so without the need for data scrubbing (Patel et al., 2014, Neuroimage). Wavelet denoising is implemented with Ameera Patel's Brain Wavelet toolbox (http://www.brainwavelet.org). The 13-parameter regression of motion and CSF signals was achieved using AFNI 3dBandpass with the -ort argument. To further characterize and describe motion and its impact on the data, we computed framewise displacement and DVARS (Power et al., 2012, Neuroimage). Examples of how denoising impacts high and low motion subjects can be found in the Supplementary Material. Between-group comparisons showed that both groups were similar with respect to motion (framewise displacement) ($F(1,97) = 2.48$, $p = 0.1183$, Cohen's $d = 0.1701$). Furthermore, mean DVARS measurements were similar across all groups before ($F(1,97) = 2.08$, $p = 0.1523$, Cohen's $d = 0.4529$) and after denoising ($F(1,97) = 0.39$, $p = 0.5363$, Cohen's $d = 0.1073$). Both of these results indicate that motion did not asymmetrically affect one group more than the others.

Next, a seed-based approach was used to calculate, for each subject, the correlation between the average timecourse of each seed with that of every other seed. Seed regions of interest (ROIs) used for the functional connectivity analyses were based on a comprehensive cortical parcellation map derived from a resting state boundary mapping technique (Gordon et al., 2014). This map divides the cortex into 333 parcels whose resting state BOLD signal is maximally distinct from their neighbors'. They also used a network detection technique referred to as Infomap (Rosvall & Bergstrom, 2008; Fortunato, 2010) to categorize each of their parcels into one of eleven networks. Using these 333 Gordon ROIs, we created a custom set of seed ROIs, many of which represented a consolidation of some smaller, neighboring parcels. This was accomplished by consolidating parcels from the same network that shared a border with each other. This resulted in 64 seed regions belonging to one of nine different networks, including auditory, cingulo-opercular, default mode, dorsal attention, frontoparietal, retrotemporal-splenial, somatomotor, ventral attention, and visual networks (**Figure 1**).

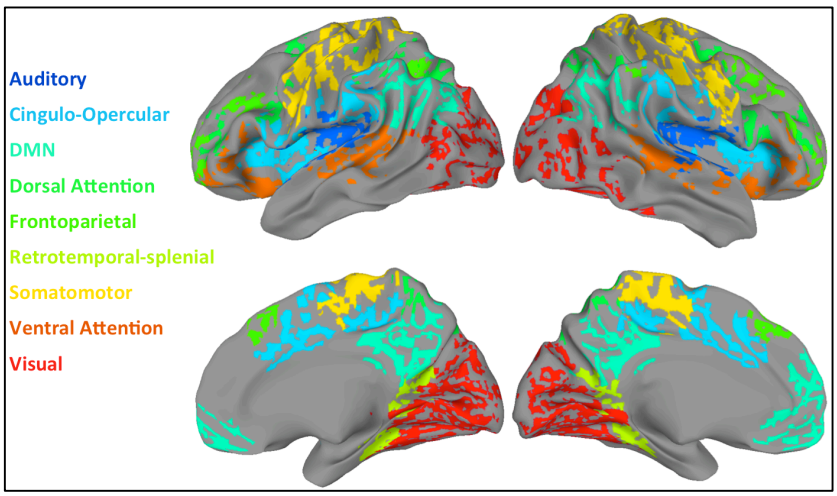

Figure 1. Networks of parcels used as seed regions for functional connectivity analyses. Cortical regions belonging to each network, based

on consolidated parcels originally created by Gordon and colleagues (2014).

Average time courses of the BOLD signal for each participant's resting state scan were obtained for each of the 64 seed ROIs. Pairwise correlations were obtained for the signal between each possible pair of seeds, for a total of 2016 pairs. Even though the groups were well matched for both age and sex, linear regression was used to eliminate any remaining variability associated with these factors from the pairwise signal correlations. The global signal was not removed from the individual ROI time series, based on findings that this signal may contain clinically relevant information (Hahamy et al., 2016).

To ensure that any effects we observed in our final analyses were not simply related to an idiosyncrasy of one particular set of ROIs, we also performed analyses with the full set of 333 ROIs from the Gordon parcellation, as well as with a set of 264 spherical ROIs based on work by Powers and colleagues (2011). Figures and results for these complementary ROI sets can be found in the Supplement.

Summary Of Main Results from Datko et al Study

1. Within- and between-network functional connectivity

A preliminary analysis looked at whether correlations between each pair of networks differed between ASD and TD. We categorized each of the 2016 possible pairwise correlations between the 64 seed ROIs by the network or networks to which each of its two ROIs belonged. We then averaged all the pairs for which each seed was part of the same network. For instance, all pairs that contained one seed in the DMN and one seed in the auditory network were included in the average for DMN-auditory connections.

Connections for which both ROIs were part of the same network were defined as within-network connections (WNC) for that network, whereas connections for which each ROI belonged to a different network from the other were defined as between-network connections (BNC), relative to the network of the first ROI of the pair (**Figure 2**). To look for overall effects of within- or between-network connectivity, we performed two ANOVAs with group (two levels, ASD and TD) and network (nine levels, each of nine networks) as factors. The first of these ANOVAs used WNC strength as the dependent variable, whereas the second used BNC strength.

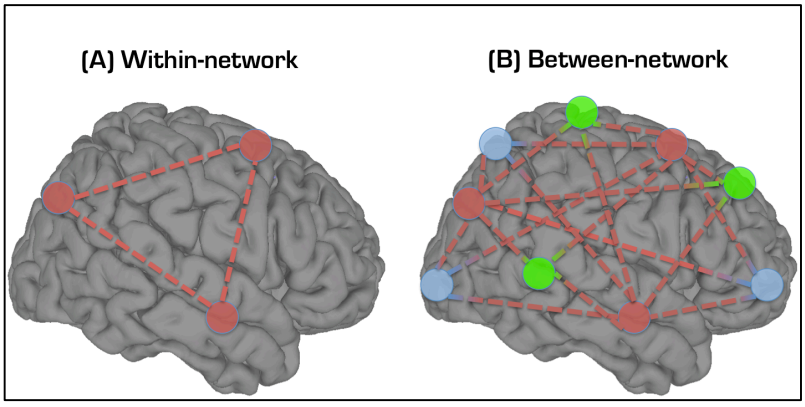

Figure 2. Components of the within-network bias ratio measure. (a) The within-network component consists of the average connection strength of all node pairs within a network (all red connections). (b) The between network component is the average connection strength of all node-pairs where the nodes are members of different networks (red to green and red to blue connections).

A preliminary analysis tested whether functional connectivity between each pair of networks differed between ASD and TD. No significant group differences in network pairwise connection strength were found for any network pairs. Correlation matrices of average pairwise network connection strengths for each group are shown in **Figure 3**.

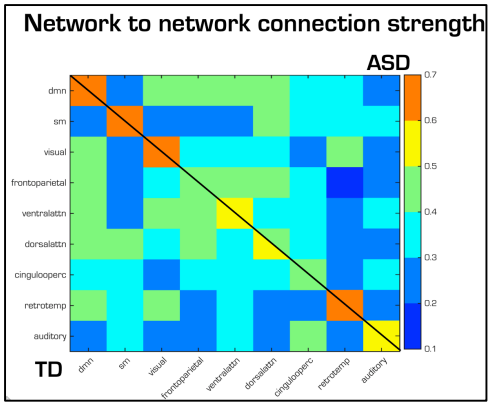

Figure 3. Correlation matrix of pairwise network connection strength. TD in bottom left triangle and ASD in top right triangle.

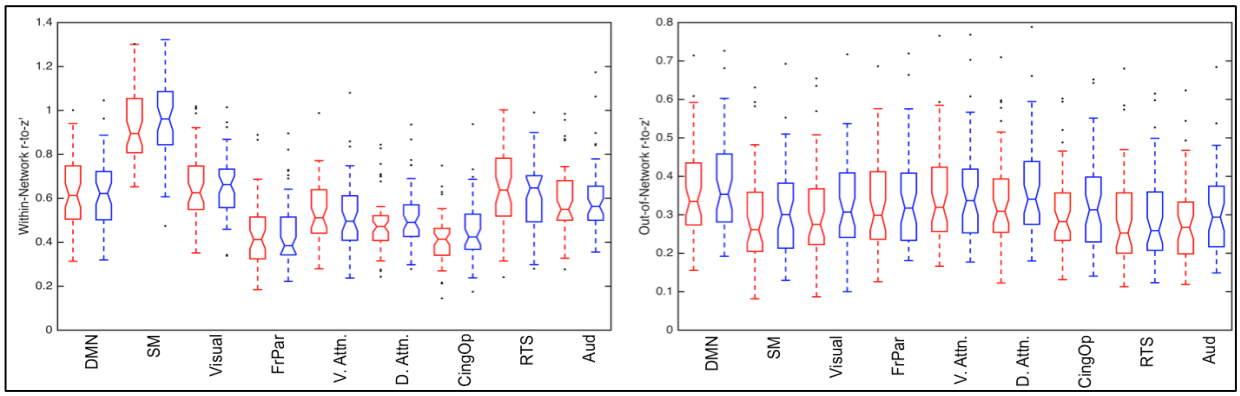

Figure 4. Within-network (left) and Between-Network (Out-of-Network) (right) connectivity for each of nine networks. ASD = Red, TD = Blue. DMN = default mode network; SM = Somatomotor; FrPar = frontoparietal; V.Attn = Ventral Attention; D.Attn = Dorsal Attention; CingOp = Cingulo-opercular; RTS = retrotemporal-splenial; Aud = auditory.

In an ANOVA using within-network connection strengths as the dependent variable, ASD and TD as the two levels of one independent factor, and each of the nine networks as levels in another factor, we found a significant main effect of network ($F_{1,8}$ = 100.13, p<0.001), but neither a main effect of group ($F_{1,8}$ = 0.43, p=0.514) nor a significant interaction ($F_{1,8}$ = 0.67, p=0.721) (**Figure 4**). In a similar ANOVA using the between-network connection strengths, there were significant main effects of group ($F_{1,8}$ = 5.23, p=0.023) and network ($F_{1,8}$ = 5.5, p<0.001), but no significant interaction ($F_{1,8}$ = 0.08, p=0.999) (**Figure 4**).

2. Seed-to-Seed Connectivity

An alternative approach to seed based functional connectivity with the 333 Gordon parcels was implemented with the Network-Based Statistics (NBS) Toolbox (Zalesky et al., 2010). First, NBS performs mass univariate t-testing at each possible connection in the matrix of seed-to-seed connections (between ASD and TD), resulting in a t-statistic for each connection. All connections whose between-group t-statistic exceeds a threshold (set by the experimenter) are admitted to a set of supra-threshold connections. Among those connections, clusters are identified in topological (as opposed to physical) space, resulting in a connected graph component for which a path can be found between any two nodes. Finally, a family-wise error rate-corrected p-value is computed for each connected graph component. This is done using permutation testing to repeat the mass univariate testing and thresholding steps, with each permutation removing a random subset of subjects from each group. A null distribution for the size of the largest component is formed consisting of the largest component from each permutation. A FWER-corrected p-value for a component of a given size is then estimated as the proportion of permutations for which the largest component was of greater or equal size."

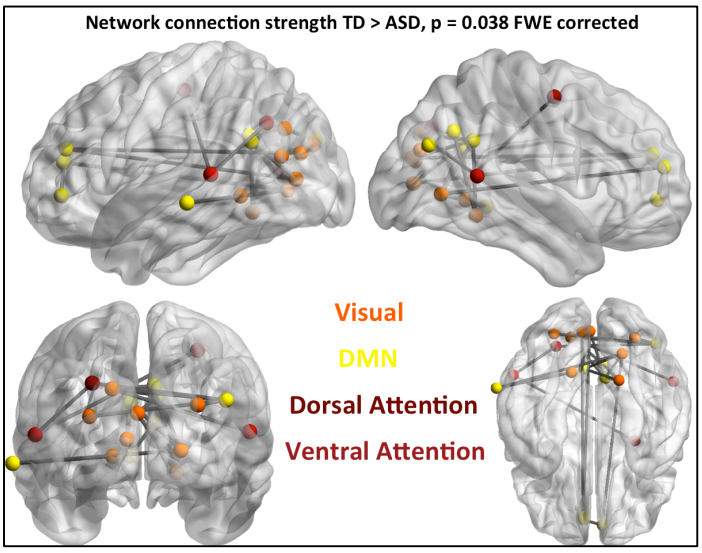

Using the NBS method, we found one graph component, consisting of 22 connections (edges) between 20 seed ROIs (nodes), in which ASD showed significantly lower connectivity compared to TD (FWER-corrected p = 0.038). Of the nodes in that component, 8 were in the default mode network, 8 were in the visual network, 2 were in the ventral attention network, and 2 were in the dorsal attention network (**Figure 5**).

Figure 5. Nodes and edges of graph component in which ASD showed significant hypoconnectivity compared to TD (FWER-corrected p = 0.038).

3. Within-network Bias

We then defined the Within-Network Bias (WNB) for a given network as the difference between WNC and BNC divided by the sum of WNC and BNC for that network. The average WNC and BNC values for each network were used to calculate WNB for each participant for each network using the formula:

$$WNB = (WNC - BNC) / (WNC + BNC)$$

Thus, WNB is the proportion of the total strength of all of one network's pairwise connections that is accounted for by the connections between only nodes of that network. Using WNB as the dependent variable, an ANOVA was performed with group (ASD and TD) and network (nine networks of interest) as independent factors.

A follow-up analysis compared the groups on a more specific measure of WNB, including only specific networks, one at a time, in the between-network component of each network's WNB ratio. We included two primary sensory networks, visual and auditory, due to the previously observed presence of strong connections within those networks even at early ages (Fransson et al., 2009, 2011; Gao et al., 2014). We also included the DMN in this analysis, due to previous studies suggesting the presence of a "proto-DMN" at early ages (Fransson et al., 2009), and due to the observation that the DMN is one of the first higher order, networks to develop "adult-like" structure in infants (Gao et al., 2009, 2014). Calculating this ratio between each combination of these networks in a pairwise fashion resulted in six different pairwise WNB values for each participant. For example, $WNB_{visual \rightarrow DMN} = (WNC_{visual} - BNC_{visual \rightarrow DMN}) / (WNC_{visual} + BNC_{visual \rightarrow DMN})$. Six between-group t-tests were used to determine if ASD and TD differed in pairwise WNB, and the resulting p-values were Bonferroni-corrected for multiple comparisons.

In an ANOVA using WNB as the dependent variable, and group and network factors identical to the previous two ANOVAs, (**Figure 6**), there were significant main effects for both the Group ($F_{1,8} = 7.92$, p=0.005) and Network ($F_{1,8} = 105.12$, p<0.001) factors, but no significant interaction between these factors ($F_{1,8} = 0.76$,p=0.642). Specifically, WNB was higher in ASD than TD groups regardless of network and WNB was highest in the sensorimotor network. In t-tests comparing the groups on a measure of specific network-pairwise WNB between the default mode, visual, and auditory networks, ASD had significantly greater WNB for $DMN_{Within} \rightarrow Visual_{Between}$ and for $Visual_{Within} \rightarrow DMN_{Between}$.

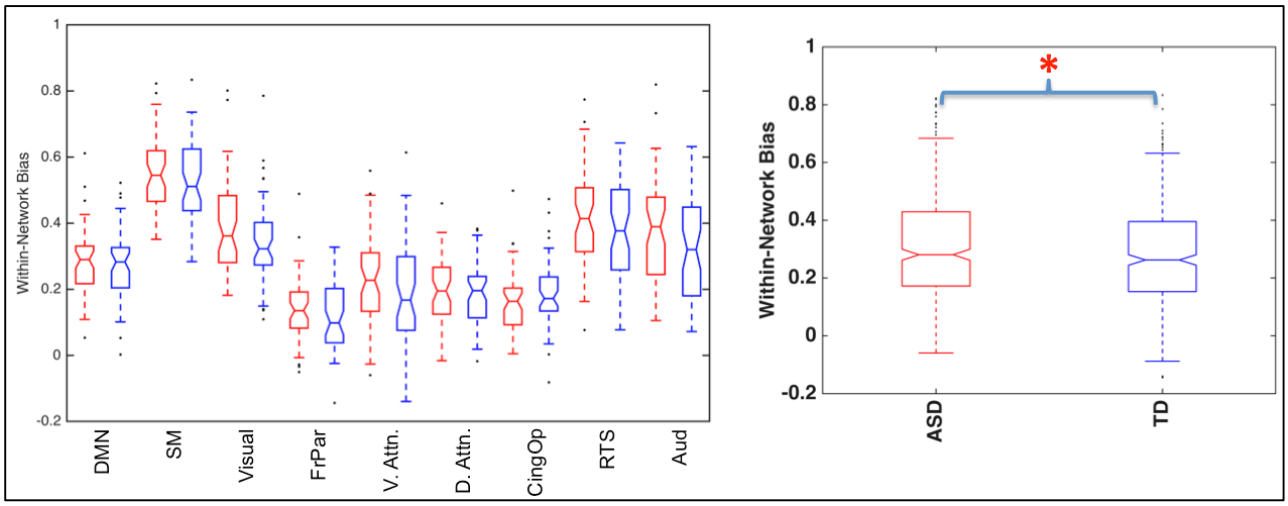

Figure 6. Within-Network Bias (WNB) for each of nine networks separately (left) and combined (right). ASD = Red, TD = Blue.

4. Age-related trajectories of Within-Network Bias

For each network, we measured the correlation between participants' WNB values and their ages. We found the Pearson correlation between these values for each group separately, and tested whether each group's correlation significantly differed from zero. We then performed a Fisher's r-to-z' transformation for each group's age-connectivity correlations. To test whether ASD and TD differed in their developmental trajectories for Within-Network Bias, we performed separate t-tests between the z' values for the two groups' age correlations. This resulted in a between-group t-score and p-value for each age correlation. ASD showed significantly different relationships, compared to TD, between age and WNB for the auditory (TD r = -0.26, TD p = 0.068; ASD r = 0.28, ASD p = 0.053; between-group p = 0.00027)

and retrotemporal-splenial (TD r = -0.20, TD p = 0.168; ASD r = 0.21, ASD p = 0.157; between-group p = 0.007) networks (**Figure 7**).

We followed this up by conducting similar between-group tests for the correlation between age and specific network-to-network WNB values, for the three networks examined in the previous section (DMN, visual, and auditory) (**Figure 7**). Among these six pairwise network WNB-age correlations, WNB appeared to increase with age in ASD but decrease with age in TD for $Auditory_W/DMN_B$, $Auditory_W/Visual_B$, and $Visual_W/Auditory_B$.

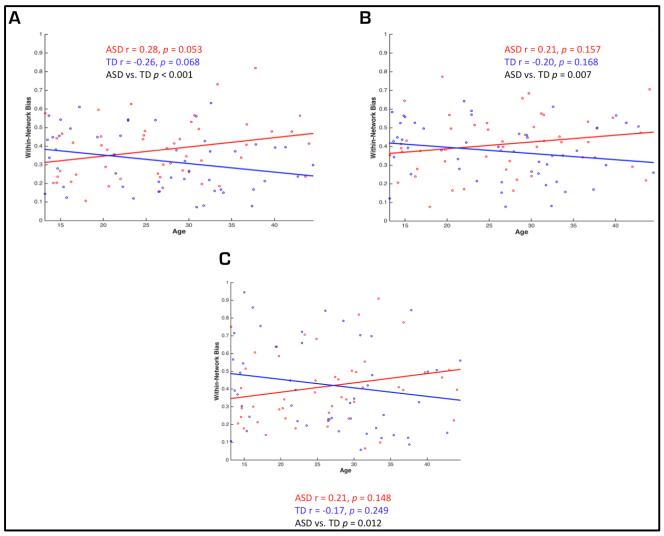

Figure 7. Significant correlations between pairwise WNB ratios and participant age.

$Auditory_{Within}/DMN_{Between}$ (A), $Auditory_{Within}/Visual_{Between}$ (B), and $Visual_{Within}/Auditory_{Between}$ (C).

LOMBARDO ET AL STUDY
(submitted, see Appendix B; references in this section in Appendix B)

Manuscript Abstract

Social orienting difficulties are central features of the first signs of ASD. However, little is known about the early atypical neurobiology behind these features and how such pathophysiology varies between individuals. Measuring visual preferences with eye tracking, we discovered that a specific subtype of ASD toddlers (termed "GeoPref" ASD; Pierce et al., 2011, 2016) who strongly or nearly exclusively attend to *non-social* dynamic geometric stimuli and ignore social stimuli, have substantially weakened functional connectivity between a key social brain network, the default mode network (DMN), and a visual network, the occipito-temporal cortex (OTC). Other ASD and developmentally delayed toddlers who prefer social stimuli do not have this DMN-OTC defect. We also found the degree of DMN-OTC disconnect in GeoPref ASD toddlers was significantly correlated with degree of neglect of real-world social interactions during the ASD "gold standard" ADOS diagnosis. This novel ASD neural-behavioral subtype also has a poor longitudinal clinical trajectory as compared to other ASD toddlers. Normally these networks work together during face-to-face social interactions and communication. Thus, DMN-OTC disconnect in GeoPref ASD toddlers may derail early experience-expectant and experience-dependent neurobiological processes that create specialized social functions during early circuit formation.

Subjects

A grand total of n=195 toddlers with valid resting state fMRI (rsfMRI) data were included in this study. Of these 195 toddlers, 109 had a diagnosis of ASD. From this total sample of 109 ASD toddlers, we identified 78 that had both valid rsfMRI data and eye tracking data from the GeoPref test (Pierce et al., 2011, 2016). These n=78 ASD individuals were included in the Discovery ASD cohort for this study, since our primary goal was to identify neural underpinnings of ASD subgroups with social orienting difficulties. The n=76 Discovery ASD participants were further divided into 2 subgroups based on their eye-tracking data. Based on our previous research, geometric responders (Geo ASD) were defined as toddlers who spent 69% or more of their time fixated on the geometric stimulus (n=16 (11 male, 5 female) mean scan age = 29.92, SD = 8.71, range = 14.16-43.79). Non-geometric responders (nonGeo ASD) were individuals who spent less than 69% of the time fixated on the geometric stimulus (n = 62 (49 male, 13 female), mean scan age = 29.37, SD = 8.35, range = 12.35-44.05). The remaining n=31 ASD toddlers (27 male, 4 female) from the total n=109 ASD individuals were held-out in a Replication dataset. These toddlers did not complete the GeoPref eye tracking test and thus Geo vs nonGeo ASD distinctions could not be made. However, they served as a Replication set for verifying case-control effects identified in the Discovery cohort. These n=31 ASD individuals were age-matched to the Geo and nonGeo ASD subgroups (mean scan age = 29.69, SD = 8.88, range = 13.21-43.63). This study also had n=86 toddlers from 3 different non-ASD comparison groups - n=55 typically-developing control toddlers (TD, 37 male, 18 female, mean scan age = 29.61, SD = 10.14, range = 13.17-47.93), n=15 language or globally developmentally delayed toddlers (LD/DD, 10 male, 5 female, mean scan age = 25.12, SD = 7.97, range = 13.37-39.75), and n=16 otherwise typically-developing toddlers who were younger siblings of children already diagnosed with ASD (TD ASDSib, 8 male, 8 female, mean scan age = 26.74, SD = 9.38, range = 12.52-44.09). An ANOVA on age at scanning found no group-differences across the groups ($F(5, 189)$ = 0.89, p = 0.48). A chi-square analysis identified a subtle trend-level difference in the proportion of males and females distributed across the sexes with more even proportions in non-ASD comparison groups ($\chi^2(5)$= 9.88, p = 0.07). In all subsequent connectivity analyses, we statistically controlled for sex and age at scanning as covariates.

Social Orienting Index and Trajectory Analyses

Using the ADOS toddler, module 1 and module 2 administrations, we computed an index of social orienting impairment by summing together items (scored 0-3, higher scores indicating more impairment) for unusual eye gaze, pointing, initiation and response to joint attention, integration of gaze during social overtures, response to name, and showing. A percentage score was then obtained by dividing this summary score by the maximum sum score possible across those items. ADOS assessment data was available for all participants longitudinally over the period of 12-55 months, allowing for analyses looking at the developmental trajectory of social orienting impairment. We used linear mixed-effect modeling analyses (modeling random slopes and intercepts) to model within-individual trajectories and group-level trajectories. These analyses were implemented with the *lme* function contained within the *nlme* library in R. A comparison of linear versus quadratic models indicated that a linear model provided a better fit (linear model, AIC = -158.09, BIC = -130.69; quadratic model, AIC = -148.64, BIC = 114.39) and thus, the linear model was used. Similar linear mixed-effect models were used across other longitudinal phenotype measures (e.g., Mullen, Vineland). For these

analyses on other clinical measures we utilized a much larger sample size of Geo ASD individuals for whom longitudinal behavioral data was available (n=60), although neuroimaging data was absent (n=44).

Resting State Imaging

See description above under the Datko et al study and Apprendix A.

FMRI Data Analysis

See description above under the Datko et al study and Apprendix A.

Connectivity Analyses

To assess functional connectivity between neural circuits in the brain we utilized the unsupervised data-driven method of independent component analysis (ICA) to conduct a group-ICA and then used dual regression to back-project spatial maps and individual time series for each component and subject. Both group-ICA and dual regression was implemented with FSL's MELODIC and Dual Regression tools (www.fmrib.ox.ac.uk/fsl). For group-ICA, we constrained the dimensionality estimate to 30, as in most cases with low-dimensional ICA, the number of meaningful components can be anywhere from 10-30 (Smith et al., 2013). Given our a priori hypotheses regarding specific processes such as social cognition, attention, salience, visual perceptive, affective, and reward processes, we examined corresponding known networks that are involved in such processes – namely, the default mode, dorsal attention, salience, several visual networks, amygdala-centered, and striatum-centered networks. Of the total 30 components, there were 14 components that best resembled such networks, and these components were included in all further analyses.

Time courses for each subject and each component were used to model between-component connectivity. This was achieved by constructing a partial correlation matrix for all 14 components using Tikhonov-regularization (i.e. ridge regression, rho=1) as implemented within the *nets_netmats.m* function in the FSLNets MATLAB toolbox (https://fsl.fmrib.ox.ac.uk/fsl/fslwiki/FSLNets). The aim of utilizing partial correlations was to estimate direct connection strengths in a more accurate manner than can be achieved with full correlations, which allow more for indirect connections to influence connectivity strength (Smith et al., 2011, 2013; Marrelec et al., 2006). Partial correlations were then converted into Z-statistics using Fisher's transformation for further statistical analyses. The lower diagonal of each subject's partial correlation matrix was extracted for a total of 91 separate component-pair comparisons. We tested each of these 91 comparisons for between-group differences in connectivity strength with a linear model implemented with the *lm* function in R, which assessed group membership as the main independent variable of interest and also covaried for sex and age at the time of scanning. F-statistics and p-values were computed based on ANOVAs for each linear model, and the p-values for the subgroup variable for each comparison were used to compute correction for multiple comparisons with FDR threshold of $q<0.05$, using the *p.adjust* function in R. Follow-up tests to identify how differences between groups manifested was achieved using pairwise t-tests and FDR $q<0.05$ correction. Effect sizes were computed as Cohen's d and were implemented with the *cohen.d* function in the *effsize* R library. For any significant differences, we further compared our distinct subgroups model to other models such as a case-control model, or continuous modeling of percentage of fixation on geometric stimuli (done within ASD groups only). Akaike information criteria (AIC) and Bayesian information criterion (BIC) statistics were used for all model comparisons and the best models were those with lower AIC and BIC values.

Case-Control Replication Analyses

Our experimental design of having independent Discovery and Replication cohorts allowed us to test for strength of replication of any identified case-control effects. To achieve this goal, we ran separate linear models (covarying for sex and age at scanning) testing for case-control differences by comparing the TD group to ASD Discovery or Replication cohorts respectively. T-statistics from these linear models were then input into code that computes replication Bayes Factor statistics, which empirically estimate strength of evidence for or against replication[80] (see here for the R code that computes replication Bayes Factors: http://bit.ly/1GHiPRe). Replication Bayes Factors greater than 10 are generally considered as strong evidence for replication.

Connectivity-Social Orienting Relationships

To test for relationships between connectivity and social orienting impairments on the ADOS, we ran computed robust regression partial correlations covarying for age at ADOS and age at scanning. Because social orienting difficulties change over development (i.e. improvement over age), we reasoned that an individual's peak of severity would be the most sensitive index of an individual's social orienting difficulties. Therefore, an individual's most severe ADOS social orienting index was selected for these analyses. However, we also tested other selections of ADOS social orienting

difficulties, such as difficulty at the time of scanning in order to show robustness of the results in this analysis. These correlations were computed using the Tor Wager's robust regression MATLAB toolbox (https://github.com/canlab/RobustToolbox) (Wager et al., 2005). To test for difference between-groups in the strength of such correlations we used the *paired.r* function in the *psych* R library to compute Z-statistics and p-values. Because correlations are point estimates and may be susceptible to effect size inflation at smaller sample sizes, we used bootstrapping to estimate variability (i.e. 95% confidence intervals) in such correlation estimates over 100,000 bootstrap resamples (i.e. *bootci.m* function in MATLAB).

Summary Of Main Results from Lombardo et al Study

Consistent ASD subtype differentiation in social orienting and other clinical measures across the first 4 years of life

In our first analysis, we set out to establish that our eye tracking GeoPref test results subtypes are meaningfully differentiated on an independent measure of real-world symptom-based social orienting difficulties. For this first proof-of-concept test, we utilized longitudinal ADOS data over 12-55 months and computed a quantitative index of real-world social orienting difficulties displayed during diagnostic testing. We utilized ADOS items tapping social orienting behaviors such as unusual eye contact, integration of gaze during social overtures, pointing, initiating and responding to joint attention, showing, and response to name. We find that GeoPref ASD has more severe social orienting impairment than nonGeo ASD across the 12-55 month age range studied (Group $F = 9.10$, $p = 0.0035$) and that these subgroups groups do not differ in the slope of their trajectories (Age-by-Group interaction $F = 0.03$, $p = 0.85$) (Fig 1D). We next behaviorally tested whether these ASD subtypes are meaningfully differentiated on other clinical measures of early language and general cognitive ability. Using a larger set of GeoPref ASD individuals (n=60) for whom longitudinal clinical data was available (but lacked rsfMRI data), we find that GeoPref ASD is consistently impaired across nearly every clinical measure we tested – ADOS social-communication, repetitive and restricted behaviors, all Mullen subscales, and all Vineland subscales except for the socialization subscale (Fig 1E-F).

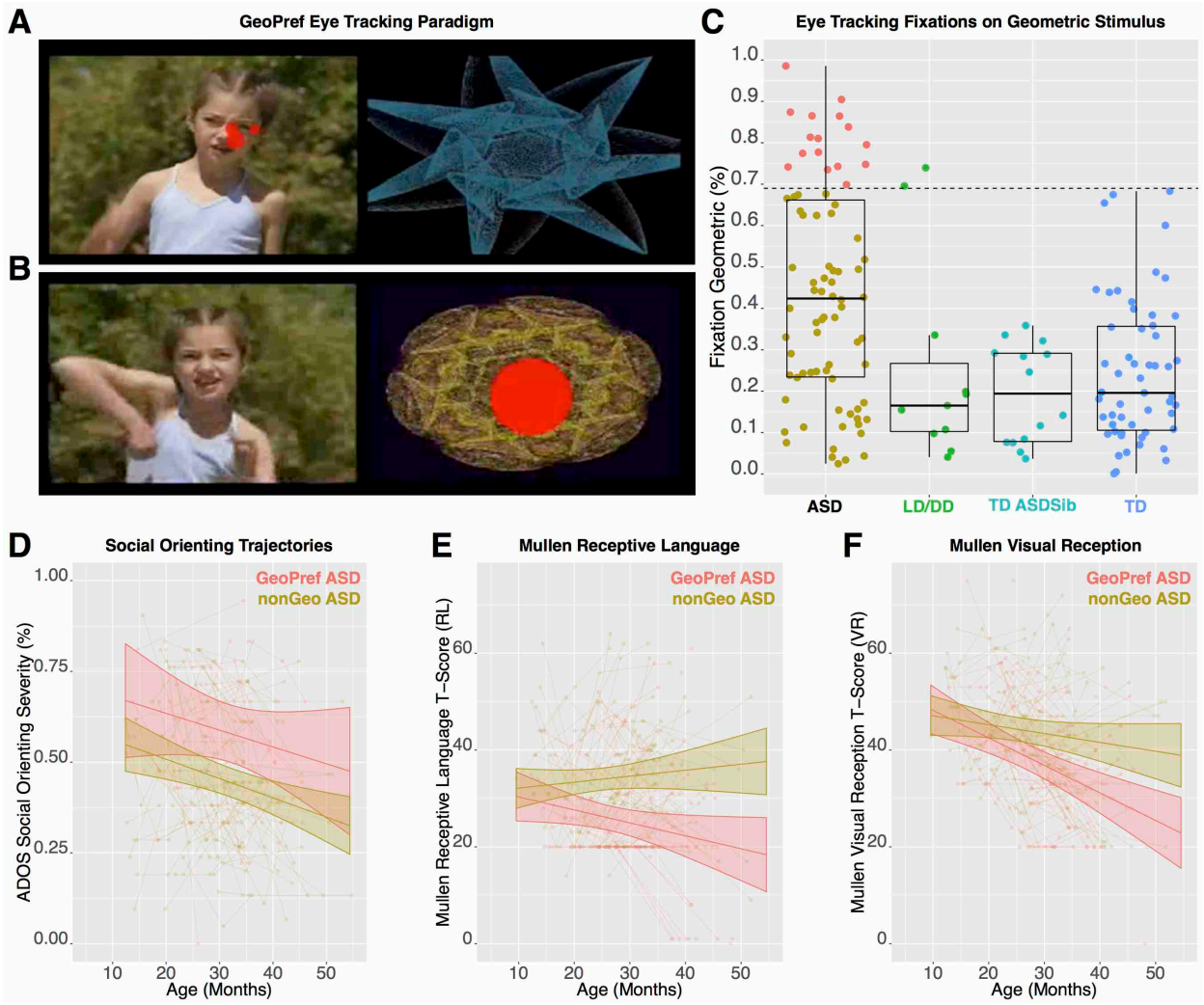

Figure 1: Behavioral differentiation on the eye tracking GeoPref test, social orienting behaviors measured by the ADOS, and Mullen language and visual scales. Panels A and B show examples of the stimuli used in the GeoPref eye tracking test. Panel A shows example fixations from an ASD individual with intact social visual preferences (nonGeo ASD), while panel B shows an example from an ASD individual with non-social visual preferences (GeoPref ASD). The red dots show visual fixations and the size of the red dots indicate fixation duration. Panel C shows eye tracking data on the GeoPref test for all groups. Percentage of time fixating on the geometric visual stimulus is plotted on the y-axis and group membership is plotted on the x-axis. The cutoff threshold of 69% is noted as the dashed line and GeoPref ASD (pink) individuals fall above the cutoff, while nonGeo ASD (gold) individuals fall below the cutoff. Panel D depicts longitudinal trajectories for a social orienting index computed from specific items from the ADOS toddler, module 1, and module 2 (e.g., unusual eye gaze, pointing, initiation and response to joint attention, integration of gaze during social overtures, response to name, and showing). Higher values on this social orienting index indicate more impairment. The GeoPref ASD subgroup is depicted in pink, while the nonGeo ASD subgroup is depicted in gold. Group trajectories and confidence bands are plotted over individual trajectory-level data depicted with transparent dots and lines. Panels E and F show trajectories on the Mullen receptive language (E) and visual reception (F) subscales.

Functional disconnection between social brain and visual circuits in GeoPref ASD

To examine our main hypothesis regarding differential neural circuit organization behind the GeoPref ASD subtype, we used group-level independent components analysis (ICA) and dual regression on rsfMRI data to identify 14 components that highly resembled *a priori* networks of interest - the default mode network, visual, dorsal attention, salience, amygdala, and striatal networks. We then used Tikhonov-regularized partial correlations (i.e. ridge regression) to model direct connections between each of the 14 components, resulting in 91 different between-component connections. Each of these between-component connections was then tested for effects of group membership via a linear model that

also covaried for sex and age at the time of scanning and significant effects were identified that passed FDR multiple comparison correction at q<0.05.

Here we discovered that only two between-component connections showed a significant between-group difference - connectivity between the social brain, default mode network (DMN), and occipito-temporal cortex (OTC) (*F(4,157)* = 5.24, *p* = 5.14e-4, *partial-*η^2 = 0.118) (Fig 2A, 2C) as well as DMN connectivity with primary visual cortex (PVC). Examining these effects from a traditional case-control standpoint, these effects manifest as reduced connectivity in ASD compared to TD. However, only the DMN-OTC effect showed high evidence in favor of replication in an independent dataset (n=31) of age-matched ASD individuals (Discovery: *t* = 3.64, *p* = 0.00039, *Cohen's d* = 0.63; Replication: *t* = 3.02, *p* = 0.0033, *Cohen's d* = 0.71; *replication Bayes Factor* = 43.54) (Fig 2B).

Although we can view the effect here as a replicable case-control difference, our main hypotheses were that the GeoPref ASD eye tracking-defined subtype may be underpinned by distinct neurobiological bases. Stopping at simple case-control effects, as is typically done in most studies, will mask deeper heterogeneity that we can uncover with knowledge of our eye tracking-defined GeoPref ASD and nonGeo ASD subtypes. Confirming our main hypothesis that these ASD subtypes are indeed underpinned by different neurobiological mechanisms, we find that driving the overall between-group difference in DMN-OTC connectivity is the GeoPref ASD subtype. Reduced connectivity between DMN and OTC is strongest in the GeoPref ASD subtype compared to nonGeo ASD (*t* = 2.65, *p* = 0.01, *Cohen's d* = 0.67) and all other non-ASD comparison groups (e.g., *Cohen's d* > 1) (Fig 2D). There was also evidence for a smaller degree of reduced connectivity in the nonGeo ASD subgroup when compared to the TD group (*t* = 2.70, *p* = 0.007, *Cohen's d* = 0.5), but not compared to the LD/DD or TD ASDSib groups (*Cohen's d* = 0.36 and 0.43, *p* > 0.05). All non-ASD groups did not differ substantially from each other (*Cohen's d* < 0.10), indicating that the overall group difference is driven by reductions in ASD, and in particular the GeoPref ASD subtype. This effect underscores a powerful effect of heterogeneity within ASD and illustrates that different neurobiology is behind the GeoPref ASD subtype.

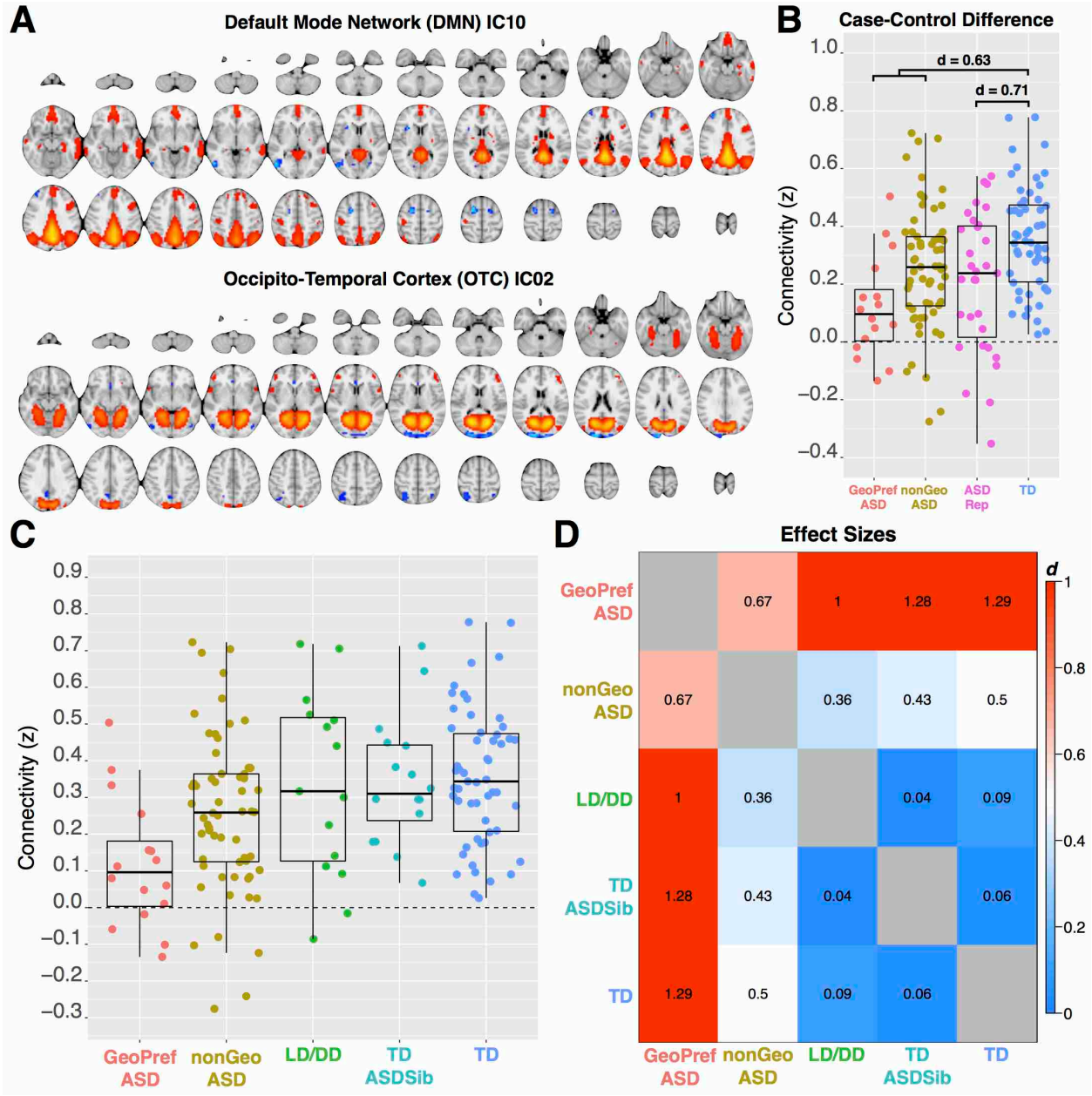

Figure 2: Enhanced functional disconnection between social brain and visual circuits in GeoPref ASD. Panel A shows axial montages of the ICA components for the social brain (default mode network; DMN) and a visual circuit within occipito-temporal cortex (OTC). Panel B shows case-control connectivity differences across the Discovery (GeoPref ASD and nonGeo ASD) and Replication datasets (ASD Rep) compared to a typically-developing (TD) comparison group. Each dot is an individual and overlaid on top of the dots is a boxplot indicating the median (solid black line), interquartile range (IQR; Q1 = 25th percentile, Q3 = 75th percentile) and upper (Q3 + (1.5*IQR)) and lower (Q1 – (1.5*IQR)) whiskers. Effect sizes for the case-control differences are shown above the boxplots. Panel C shows connectivity between components for all groups in the Discovery dataset (GeoPref ASD, nonGeo ASD, LD/DD, TD ASDSib, and TD). Panel D uses a heatmap to show effect sizes (Cohen's d) for all pairwise comparisons in the Discovery dataset. Note that effect sizes are depicted in panel D as absolute values, and the directionality of the effects can be seen in panel C.

Comparing the subtype model to case-control and continuous models

We next empirically tested whether modeling the data as two ASD subtypes indeed provided a better explanatory power over the variance compared to simpler case-control models. Using AIC and BIC model comparison statistics as measures, we find that the subtype model was indeed more optimal (i.e. lower AIC and BIC values) for characterizing DMN-OTC connectivity. In addition, we also considered whether models utilizing distinct subtype labels are better than

other models which utilize eye tracking behavior from the GeoPref test in a continuous fashion. If our subtyping scheme is indeed a better way of accounting for heterogeneity in social orienting in ASD, we should expect that such models would better account for variability in connectivity over and above conceptualizing individual differences in social orienting as a spectrum of continuous change across the entire ASD spectrum. Again, we find that AIC and BIC scores are lower for the subtype model compared to modeling social orienting via continuous behavioral variability measured from the GeoPref test (i.e. percentage fixation on the geometric stimulus in the GeoPref test).

Subtype-specific association between social brain-visual disconnection and individual-level variability social orienting difficulties

We next tested whether the two ASD subtypes would differ in the relationship between social brain-visual connectivity and social orienting difficulties. This test is critical for examining the question of whether the two ASD subtypes should indeed be considered as discrete types of ASD with different underlying neurobiological mechanisms that are differentially-relevant for the behavioral phenotype. If these are indeed distinct subtypes we expect that variability within the neurobiology (i.e. connectivity) of each subtype would be differentially associated with severity of their real-world symptom-based social orienting difficulties.

Our analyses utilized partial correlations (computed with robust regression in order to be insensitive to outlying data points) to examine the relationship between most severe ADOS social orienting index and DMN-OTC connectivity, while covarying for both age at time of ADOS and age at the time of scanning. Because we had several ADOS measurements at different timepoints to consider for this analysis, we *a priori* selected an individual's peak of social orienting impairment in order to be maximally sensitive to core behavioral impairments that may be less affected by general developmental progress (e.g., age-related improvement; Fig 1D). Correlations for each group were then formally compared to test for a between-group difference in the strength of correlation. As predicted, there was a strong negative correlation in the GeoPref ASD subgroup (r = -0.86, p = 1.91e-4), but no such relationship in the nonGeo ASD subgroup (r = 0.12, p = 0.38) (Fig 3B), and the difference in strength of correlation between-subtypes was highly significant (z = 4.74, p = 2.03e-6). Note that the observed correlation in GeoPref ASD is quite large and given the relatively small sample size of that group, it may be that this estimate overestimates the true effect[49]. Therefore, we used bootstrapping to estimate the variability in such an estimate (i.e. 95% bootstrap confidence intervals) for both ASD subgroups. As can be seen in Fig 3C, the distributions for each subgroup are highly separated (GeoPref ASD: *95% CI* = [-0.99, -0.50]; nonGeo ASD: *95% CI* = [-0.25, 0.52]), indicating that even if the observed sample estimates of correlation are overly optimistic, the effect of differentiation of correlation between the two groups is still highly robust. This effect was also robust to which timepoint of ADOS social orienting index was selected. For example, when using ADOS social orienting index at the time of scanning the results were unchanged, though the strength of the difference was slightly attenuated (GeoPref ASD, r = -0.61, *95% CI* = [-0.97, -0.23], p = 0.0251; nonGeo ASD, r = 0.03, *95% CI* = [-0.26, 0.33], p = 0.80; between-group difference, z = 2.43, p = 0.01).

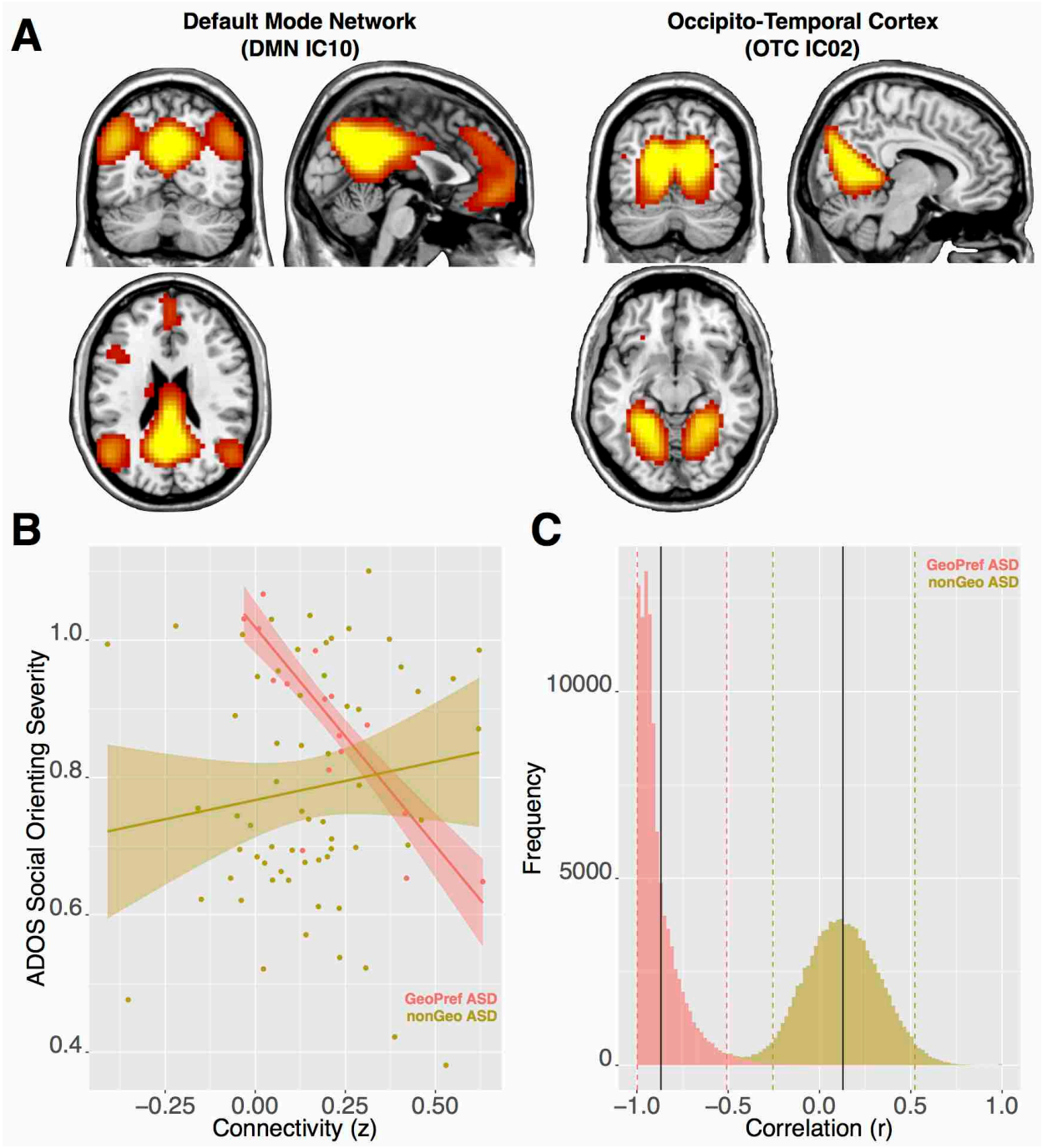

Figure 3: Subtype-specific association between social brain-visual disconnection and individual-level variability in social orienting difficulties. Panel A shows representative 3 plane views of the social brain, default mode network (DMN, IC10), and visual circuit in occipito-temporal cortex (OTC, IC02) assessed in this connectivity-social orienting relationship analysis. Panel B shows the DMN-OTC connectivity relationship with the ADOS social orienting index. The social orienting index was selected as the peak of impairment for each individual across their longitudinal dataset. Panel C shows histograms of the connectivity-social orienting relationship after 100,000 bootstrap resamples (the observed correlation is shown as the solid black line and the 95% confidence intervals are shown as dotted lines).

d. What opportunities for training and professional development has the project provided at the UC San Diego Site?

While a major goal of the project at our site was not to provide training and professional opportunities, we nonetheless were able to do so. Much of the work accomplished in the Datko et al manuscript was completed by Dr. Michael Datko, the post-doc who was hired for this project. Though he already had a background in fMRI processing and

analysis, as well as literature on ASD, he continued to grow in knowledge and professional skill in these areas and developed pipelines using advanced statistical analysis techniques involving multiple regression and mass univariate testing. Mike now has a position at Yale University.

e. How were the results disseminated to communities of interest?

They are submitted to top journals and will be published and made widely available. In addition, the P.I., Dr. Courchesne, describes them in lectures given locally, nationally and internationally.

f. What do you plan to do during the next reporting period to accomplish the goals?

N/A. The goals have been accomplished in our highly successful studies and these results in turn have been important to writing new NIH grants that have been awarded to Dr. Courchesne to continue this important line of research on ASD infants and toddlers.

These are among the first-ever studies of the intrinsic connectivity patterns in infants and toddlers with ASD at the age of first clinical identification.

4. IMPACT

a. What is the impact on understanding ASD brain development of the project?

Our initial intrinsic connectivity analyses of ASD at the age of first clinical diagnosis provides evidence of significant and widespread disruptions in the functional networks that are crucial for basic sensory and higher-order social cognitive functions (**Section 3. ACCOMPLISHMENTS**, above).

In our first study, Datko et al (submitted, see Appendix A), we found evidence for a bias towards within-network connectivity in ASD infants and toddlers. Over all the networks examined, although not in any particular network, we found that stronger within-network connections accounted for significantly more of the total connection strength compared to between-network connections, in the ASD group compared to the TD group. All networks for both groups showed positive WNB values, indicating that, as expected, within-network connectivity was universally stronger than between-network connectivity. This was particularly true for primary sensory networks, including those supporting sensorimotor, visual, and auditory functions.

In Datko et al (submitted, see Appendix A), the global effect of higher WNB in our ASD sample suggests that early brain networks in ASD are perhaps more isolated than would be expected for a developmental period that has previously been characterized by a balance between increasing within-network connectivity alongside the development of more interregional connections. Gao and colleagues (2014) found during the first two years of life, typical infants showed greater within-network connectivity and a mix of increased and decreased between-network connectivity. Whether any two networks became more or less functionally segregated from each other during this period depended on the functional and developmental relationship between them. However, the age range of our sample only partially overlaps with the younger range of Gao's study. While they observed the strongest changes in functional connectivity over the period from birth to 12 months of age, with only modest changes from 12 to 24 months, our sample's ages range from 12 to 48 months.

Our Datko et al. (submitted, see Appendix A) finding of globally increased WNB is also a sharp contrast to studies of ASD adolescents and adults who show reduced within-network integration (i.e., hypoconnectivity) and reduced between-network segregation (i.e., hyperconnectivity) (Rudie et al., 2012). One possible explanation is that in adolescents and adults, the process of synaptic pruning and network maturation has been dysregulated for years, resulting in an excess of connections between networks which would typically have developed more distinct, segregated functional properties. But the first stages of that process involve an early overgrowth of connections, possibly manifesting at the level of functional connectivity as the within-network bias we have reported here.

Using the Network-Based Statistic developed by Zalesky and colleagues (2010), in our Datko et al (submitted, see Appendix A) study, we also found a connected graph component, consisting of seeds from 4 different networks, that showed significantly lower functional connectivity in ASD compared to TD participants. Notably, most of the connections in this component were between nodes of the visual and default mode networks, with a small number of nodes also belonging to the dorsal and ventral attention networks. While the DMN has received substantial attention in the adolescent and adult ASD literature, with many studies reporting atypical patterns of functional activation and

connectivity (Assaf et al., 2010; Lynch et al., 2013; Starck et al. 2013; Washington et al., 2014), this is the first study to show hypoconnectivity between and within the DMN and visual networks in infants and toddlers with ASD. Since the primary visual network is one of the first to have a functional organization resembling that seen in adults, our findings indicate that disrupted connectivity between primary sensory (visual) and early higher-order (DMN) networks may cause downstream effects on the dynamics of other higher order networks such as those involved in social cognition and executive function.

Our first study, then, suggested that atypical DMN function in ASD adults originates not from a gradual process of being shaped by environmental and behavioral influences throughout development (Johnson, 2000), but rather more directly follows Gottlieb's model of "predetermined epigenesis" (1992).

In our second study ---Lombardo et al (submitted, see Appendix B), we therefore tested this specific hypothesis of disconnection between the DMN social network and visual sensory processing networks by comparing GeoPref responders who ignore social visual stimuli and Social Responders who do look at social visual stimuli using data from our GeoPref ASD Test.

With this design in Lombardo et al (submitted, see Appendix B), we were able to address the neural bases of social orienting difficulties in ASD at the age first clinical detection. This has high clinical and translational relevance because social attending and responding are central to ASD. And the neural bases have remained shrouded in mystery. Using our innovative paradigm that captures social orienting deficits and their heterogeneity in ASD at very young ages (Pierce et al., 2011, 2016), we discovered that GeoPref ASD toddlers who strongly or nearly exclusively attend to non-social dynamic geometric stimuli and ignore social stimuli, have substantially functionally disconnected neural circuits involved in higher-order social cognitive and social-communicative processes (i.e. DMN) and visual perception (i.e. OTC). Importantly, this enhanced functional disconnection between DMN and OTC specific to GeoPref ASD was associated with individual-level variability in real-world symptom-based social orienting difficulties taken from an ASD 'gold standard' diagnostic instrument (i.e ADOS). Thus, extreme DMN-OTC disconnect and its clinical impact are highly specific to GeoPref ASD toddlers. This brain-behavior relationship may be key to understanding this ASD subtype. It is known that DMN social and visual networks specifically enhance their effective connectivity in the mature adult brain during periods of eye-contact compared to viewing a person's mouth while watching and listening to the verbal social communications of others[50]. It could be that this specific early functional disconnection between social brain and visual circuits in GeoPref ASD has important impact on further developmental functional specialization of the social brain for social cognitive and social-communicative functions.

It is unknown what neurobiological processes underlie the macroscale circuit-level DMN-OTC disconnection in GeoPref ASD toddlers. However, it is clear from our new DoD-supported review (Courchesne et al., submitted; see Appendix C) that neural pathophysiology in ASD likely begins in prenatal periods of development (Courchesne et al, 2011; Parikshak et al., 2013, 2016; Willsey et al., 2013; Marchetto et al., 2016). This prenatal pathophysiology is diverse but includes increased cell proliferation, aberrant cell migration, and downregulated early axonogenesis during early prenatal periods, whereas starting in later prenatal development and continuing postnatally throughout the first years of life there are also downregulation of processes typically important for synapse development (Courchesne et al., submitted; see Appendix C). We have long theorized that such early abnormalities could cause disconnection of higher-order frontal social and communication networks from lower-level posterior perceptual networks and thereby impair attention to and integration of relevant social, emotional and communicative events during development in ASD (Courchesne and Pierce, 2005). While these early developmental abnormalities are numerous and diverse, a key goal for future work will be to determine which processes, or collection of processes working together, lead to the GeoPref ASD subtype. One compelling hypothesis is that prenatal pathophysiology in GeoPref ASD could cause a cascade in early development leading towards the ultimate initiation of atypical social orienting behaviors. The emergence of early social orienting difficulties in the GeoPref ASD subtype could be considered as an early adaptation response by the developing brain to very atypical prenatal neurobiological starting points (Johnson et al., 2015; Johnson 2017) Thus, it will be crucial for future work to examine what might be the early prenatal pathophysiology underpinning this subtype and how it may be linked to individual differences in later social orienting difficulties. Work utilizing induced pluripotent stem cell (iPSC) modeling to recapitulate some of the early prenatal neurobiological processes occurring in such individuals seems highly appropriate for beginning to answer such questions (Marchetto et al., 2016).

Theoretically it is important to discuss how the findings here are relevant to early developmental functional specialization of social brain circuitry within GeoPref ASD. Atypical early social orienting behaviors that are adaptations to early atypical prenatal starting points could potentially lead to the construction and long-term maintenance of atypical early developmental environmental niches for an individual (Pierce et al., 2011, 2016). An environmental niche

constructed and maintained from largely sampling the non-social instead of the social world around an infant could have large impact on how postnatal neural circuits are formed. It is well known that neural circuits are sculpted by experience, particularly in the early years of life when biological processes such as synaptogenesis, axon expansion, and cell-growth are normally at their peak (Greenough et al., 1987; Holtmaat & Svoboda, 2009; Huttenlocher, 2002; Kang et al., 2011). Selective biases to the type of information sampled from the environment in GeoPref ASD may provide the wrong type of input to facilitate social cognitive and social-communicative functional specialization of circuits such as the DMN. Circuits such as the DMN undergo protracted developmental periods of interactive specialization (Johnson, 2011), whereby specialization is achieved through interactions between circuits. Our work here suggests that functional interaction between visual and social brain circuits may be crucial to early social behavior in the GeoPref ASD subtype, and may have further impact for aiding the developing specialization of function within social brain circuitry.

In addition to showing that GeoPref ASD is neurobiologically underpinned by functional disconnection between social brain and visual circuits, we have also added to our previous findings (Pierce et al., 2011, 2016) suggesting that this ASD subtype also is highly clinically relevant in their generally poorer developmental trajectories and outcome across a range of different domains. Given our findings, the next clinically-relevant question becomes whether these toddlers may be responsive to early treatment. Under one view, it could be that early prenatal neurobiological abnormalities set up neurobiological architecture that is resistant to postnatal experience-dependent changes typically capitalized on by early intervention. However, an alternative view could be that the neurobiological abnormalities in this subtype are not 'hardwired' and could be changed if appropriate early intervention is set into place to correct for the lack of social input to developing social brain systems like the DMN. Future work will be needed to answer this question and, hopefully, discover what types of early intervention programs can lead to optimal outcomes.

In conclusion, the GeoPref ASD subtype is a distinct ASD subtype of high translational and clinical importance and which can be identified with high levels of precision via a simple eye tracking test of social or non-social visual preferences in very early development. Here we have discovered that GeoPref ASD toddlers have a functional disconnection of the DMN, a core social network, from OTC, a core visual network that explains their striking difficulties in visual orienting to the social world. This disconnection of social and visual circuits occurs during a developmental period when *increased* connectivity is the neurobiological expected norm. A biologically driven bias (particularly from prenatal development) leading towards neglect for the social world in early development, if left untreated, would significantly diminish opportunities for social learning and for bootstrapping experience-dependent change within developing neural circuits. This, we suggest, may limit developmental functional specialization within the social brain and lead towards more permanent long-term social, language and cognitive disability. Therefore, it is an important goal to hone in on early-age molecular biomarkers of risk for this ASD subtype since very early identification may have large clinical and translational benefits for the child. Early detection and interventions that successfully ameliorate this disconnection might improve social development and outcome for these ASD individuals. Despite the narrow view of some institutions (USPSTF), early risk detection is an absolute necessity (Pierce et al., 2016) as is research to devise effective early GeoPref ASD-specific interventions.

b. What was the impact of the project results on other disciplines, technology transfer, or society beyond science and technology?

See above **Impact** section.

5. CHANGES/PROBLEMS

No scientific, design or experiment problems occurred at the UC San Diego site. The most significant staffing task completed was the hiring of Dr. Datko as a full-time postdoc to work on this project. We completed processing of MRI structural and fMRI resting state data from large samples of ASD and TD infants and toddlers as planned and we completed two resting state fMRI studies that are the first of their kind on ASD infants and toddlers in two large sample studies, one with n=98 and the other with n=195 infants and toddlers. The research is complete and was highly successful

6. PRODUCTS

Three manuscripts are currently submitted and in review: Datko et al, Lombardo et al., and Courchesne et al. Please see Appendices A, B, and C.

7. PARTICIPANTS AND OTHER COLLABORATING ORGANIZATIONS

At the UC San Diego Site, Dr. Eric Courchesne who is Site P.I., Dr. Lisa Eyler and Dr. Michael Datko have worked on the project here.

8. SPECIAL REPORTING REQUIREMENTS

This is part of a Collaborative Award and this Progress Report is from the UC San Diego Site (Courchesne).

9. NUMBERED REFERENCES for Page 2, Introduction

NUMBERED REFERENCES FOR INTRODUCTION on Page 2

1. Damaraju E, Phillips JR, Lowe JR, Ohls R, Calhoun VD, Caprihan A. Resting-state functional connectivity differences in premature children. *Front Syst Neurosci.* 2010;4.
2. Fransson P, Skiold B, Horsch S, et al. Resting-state networks in the infant brain. *Proc Natl Acad Sci U S A.* 2007;104(39):15531-15536.
3. Fransson P, Aden U, Blennow M, Lagercrantz H. The functional architecture of the infant brain as revealed by resting-state fMRI. *Cereb Cortex.* 2011;21(1):145-154.
4. Smyser CD, Inder TE, Shimony JS, et al. Longitudinal analysis of neural network development in preterm infants. *Cereb Cortex.* 2010;20(12):2852-2862.
5. Doria V, Beckmann CF, Arichi T, et al. Emergence of resting state networks in the preterm human brain. *Proc Natl Acad Sci U S A.* 2010;107(46):20015-20020.
6. Gao W, Zhu H, Giovanello KS, et al. Evidence on the emergence of the brain's default network from 2-week-old to 2-year-old healthy pediatric subjects. *Proc Natl Acad Sci U S A.* 2009;106(16):6790-6795.
7. Gao W, Gilmore JH, Giovanello KS, et al. Temporal and spatial evolution of brain network topology during the first two years of life. *PLoS One.* 2011;6(9):e25278.
8. Gao W, Gilmore JH, Shen D, Smith JK, Zhu H, Lin W. The synchronization within and interaction between the default and dorsal attention networks in early infancy. *Cereb Cortex.* 2013;23(3):594-603.
9. Gao W, Alcauter S, Smith JK, Gilmore JH, Lin W. Development of human brain cortical network architecture during infancy. *Brain Struct Funct.* 2015;220(2):1173-1186.
10. Avino TA, Hutsler JJ. Abnormal cell patterning at the cortical gray-white matter boundary in autism spectrum disorders. *Brain research.* 2010;1360:138-146.
11. Courchesne E, Mouton PR, Calhoun ME, et al. Neuron number and size in prefrontal cortex of children with autism. *JAMA.* 2011;306(18):2001-2010.
12. Chow ML, Pramparo T, Winn ME, et al. Age-dependent brain gene expression and copy number anomalies in autism suggest distinct pathological processes at young versus mature ages. *PLoS Genet.* 2012;8(3):e1002592.
13. Willsey AJ, Sanders SJ, Li M, et al. Coexpression networks implicate human midfetal deep cortical projection neurons in the pathogenesis of autism. *Cell.* 2013;155(5):997-1007.
14. De Rubeis S, He X, Goldberg AP, et al. Synaptic, transcriptional and chromatin genes disrupted in autism. *Nature.* 2014;515(7526):209-215.
15. Stoner R, Chow ML, Boyle MP, et al. Patches of disorganization in the neocortex of children with autism. *N Engl J Med.* 2014;370(13):1209-1219.
16. Fang WQ, Chen WW, Jiang L, et al. Overproduction of upper-layer neurons in the neocortex leads to autism-like features in mice. *Cell reports.* 2014;9(5):1635-1643.
17. Orosco LA, Ross AP, Cates SL, et al. Loss of Wdfy3 in mice alters cerebral cortical neurogenesis reflecting aspects of the autism pathology. *Nature communications.* 2014;5:4692.
18. Le Belle JE, Sperry J, Ngo A, et al. Maternal inflammation contributes to brain overgrowth and autism-associated behaviors through altered redox signaling in stem and progenitor cells. *Stem cell reports.* 2014;3(5):725-734.
19. Courchesne E, Webb SJ, Schumann CM. *From toddlers to adults: The changing landscape of the brain in autism.* USA: Oxford University Press; 2011.

20. Redcay E, Courchesne E. Deviant functional magnetic resonance imaging patterns of brain activity to speech in 2-3-year-old children with autism spectrum disorder. *Biol Psychiatry.* 2008;64(7):589-598.
21. Dinstein I, Pierce K, Eyler L, et al. Disrupted neural synchronization in toddlers with autism. *Neuron.* 2011;70(6):1218-1225.
22. Wolff JJ, Gu H, Gerig G, et al. Differences in white matter fiber tract development present from 6 to 24 months in infants with autism. *Am J Psychiatry.* 2012;169(6):589-600.
23. Eyler LT, Pierce K, Courchesne E. A failure of left temporal cortex to specialize for language is an early emerging and fundamental property of autism. *Brain.* 2012;135(Pt 3):949-960.
24. Lombardo MV, Pierce K, Eyler LT, et al. Different functional neural substrates for good and poor language outcome in autism. *Neuron.* 2015;86(2):567-577.
25. Solso S, Xu, R., Proudfoot, J., Hagler, D.J., Campbell, K., Venkatraman, V., Carter Barnes, C., Ahrens-Barbeau, C., Pierce, K., Dale, A., Eyler, L., Courchesne, E. DTI Provides Evidence Of Possible Axonal Over-Connectivity In Frontal Lobes In ASD Toddlers. *Biol Psychiatry.* in press.

APPENDICES A, B AND C